Capacitor Selection Method in PV Interfaced Converter Suitable for Maximum Power Point Tracking

Bikash Santra, Subhendu ; Chatterjee, Debashis ; Kumar, Kundan; Borteluzzo, Manuele; Sangwongwanich, Ariya; Blaabjerg, Frede

Published in:
IEEE Journal of Emerging and Selected Topics in Power Electronics

DOI (link to publication from Publisher):
10.1109/JESTPE.2020.2986858

Publication date:
2021

Document Version
Accepted author manuscript, peer reviewed version

This article has been accepted for publication in a future issue of this journal, but has not been fully edited. Content may change prior to final publication. Citation information: DOI 10.1109/JESTPE.2020.2986858, IEEE Journal of Emerging and Selected Topics in Power Electronics

Capacitor Selection Method in PV Interfaced Converter Suitable for Maximum Power Point Tracking

Subhendu Bikash Santra[1], *Member IEEE*, Debashis Chatterjee[2], Kundan Kumar[1], *Member IEEE*, Manuele Borteluzzo[3], Ariya Sangwongwanich[4], *Member IEEE*, Frede Blaabjerg[4], *Fellow, IEEE*

[1]School of Electrical Engineering, KIIT University, [2]Department of Electrical Engineering, Jadavpur University, [3]Department of Industrial Engineering, University of Padova, Italy, [4]Department of Energy Technology, Aalborg University, Aalborg DK-9220, Denmark

***Abstract*—Capacitor is connected primarily between photovoltaic (PV) panel and power electronics converter (PEC) to suppress input voltage ripple and filter ripple current. However, this capacitor creates an error in maximum power point tracking (MPPT) for a fixed step algorithm under rapidly changing environmental condition if not selected properly. Therefore, the capacitor value selection along with maximum sampling rate determination is crucial for achieving error-free MPPT. A comprehensive analysis is carried out to prove the dependency of capacitor value on MPPT performance under irradiation and temperature variation. The analysis also includes the effect of ripple power on capacitor value selection when PV interfaced converter is connected to the grid. Finally, the capacitor value and the sampling rate of PV interfaced power electronics converter is determined. Simulation and experimental results confirm the theoretical findings.**

***Index Terms*— Maximum Power Point Tracking (MPPT), Capacitor, PV interfaced Converter.**

I. Introduction

Power electronics converters (PEC) are interfaced in the configurations of photovoltaic (PV) power generation system [1]. Generally, a capacitor is connected between the PV panel and power converter to filter voltage ripple and current ripple so that ripple content will not affect the PV panel [1]. There are three regions of operation of PV sources i.e. constant current region, constant voltage region, and constant power region [2]. Constant power region is the required mode of operation for extracting maximum power from the PV panel. Different MPPT algorithms [2] are found in the literature to ensure PV operation in the constant power region. In the static or slow environmental change conditions PV panel voltage and current do not change much and therefore these MPPT algorithms can operate accurately. The selection of capacitance is not important in a static condition. However, these algorithms perform inaccurately under dynamic environmental conditions [3] as they rely on the voltage and current sensing information. PV panel voltage changes with irradiation `variation operated in MPP condition as shown in Fig. 1.

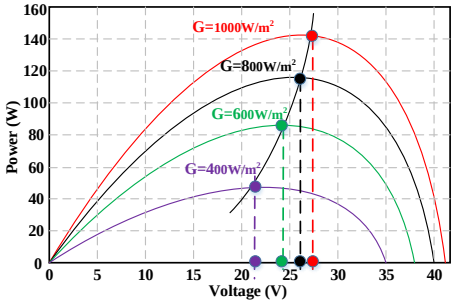

Fig. 1 PV voltage change at MPP with irradiation (G) variation.

The capacitor voltage does not change immediately with irradiation variation due to circuit time constant. Again, the sensing and processing delay of the algorithm takes additional time. These delays in PV system should be as small as possible for tracking error-free MPP operation. Several advanced control techniques [4-5] are proposed by researchers to track reference power changes accurately with irradiation and temperature variation. There are two approaches i.e. using (a) advanced control technique (b) low capacitance value to optimize settling time [6], found in the literature to extract maximum power from PV under rapidly changing environmental conditions. Different adaptive control techniques like FPPT as proposed by H.D. Tafti *et.al*. [7] using modern digital signal processor (DSP) confirms good MPP operation under sudden irradiation change. Again, multi-mode FPPT is proposed by H.D. Tafti *et.al*. [8], where small adjustment in voltage is processed in controller to achieve fast dynamics. For multi-string structure under inhomogeneous irradiation maximum power point tracking error is nullified by time-sharing MPPT [9] technique. This problem is also addressed by S. Selvakumar *et.al*. [10], where the fast determination of global maximum power point (GMOP) is achieved in conjunction with a boost converter.

However, capacitor selection-based solution to minimize settling time for error-free point tracking is not yet explored which is simple and cost-effective. Capacitor selection based on PV microinverter [11-13] does not concentrate on the impact of capacitance for MPP operation. Lowering the perturbation period compared to system setting time can improve MPPT performance but it increases steady-state oscillation. The correct capacitance value between the PV panel and PEC with accurate perturbation time can eliminate error in MPPT performance in varying conditions.

Therefore, the novelties of this work are the following.

(1) Impact of PV panel parameter and capacitance value on MPPT.
(2) Effect of ripple power on capacitance selection.
(3) Minimization of settling time which allows low perturbation frequency operation and error-free MPPT on dynamic environmental conditions.

The paper is organized as follows: Section II elaborates the system configuration and their dynamics. Sections III expounds the methods of capacitor selection while the various results and detail discussion are presented in Section IV. Finally, paper concludes in Section V.

II. System Configuration and Dynamics

Boost converter is selected as PV interfaced PEC for analyzing and testing the effects of output capacitance (C_f) on MPPT. The configuration is shown in Fig. 2. Simple perturbation-based technique (P and O) is considered to extract MPP from PV panel in this work because it is simple and effective [1], [14].

This article has been accepted for publication in a future issue of this journal, but has not been fully edited. Content may change prior to final publication. Citation information: DOI 10.1109/JESTPE.2020.2986858, IEEE Journal of Emerging and Selected Topics in Power Electronics

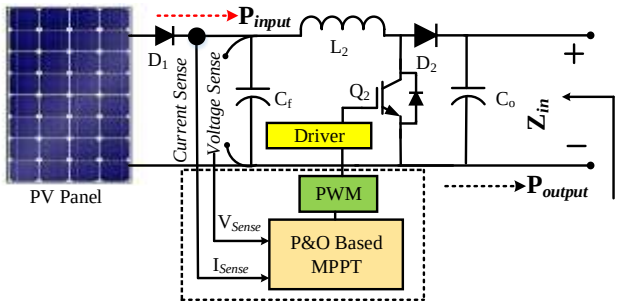

Fig. 2. PV system with boost converter.

Sensed voltage and current signal from a solar PV panel is essential for duty ratio determination of boost converter to extract maximum power. When irradiation changes at loaded condition, the capacitor (C_f) voltage, i.e., the PV panel voltage, should change to a new value as per Fig. 1 immediately. However, the circuit time constant introduced by the capacitor between the PV panel and the boost converter, C_f, restricts the immediate voltage change as shown in Fig. 3. This time delay is considered as source side time constant delay in this work. This delay together with the time required to sense the capacitor (C_f) voltage V_f, PV current and the processing time create an additional delay. Therefore, the total time delay considered while analyzing the performance of maximum power point extraction under irradiation change is the combination of source-side time constant delay and sensing-processing delay.

The quantity P_{K1} in Fig. 3 represents the reference power from PV and P_{Ka1} is the actual power after implementing the MPPT algorithm. Slow rate irradiation change with minimum delay ensures constant power region or MPPT operation and considered as ideal case as shown in Fig. 3.

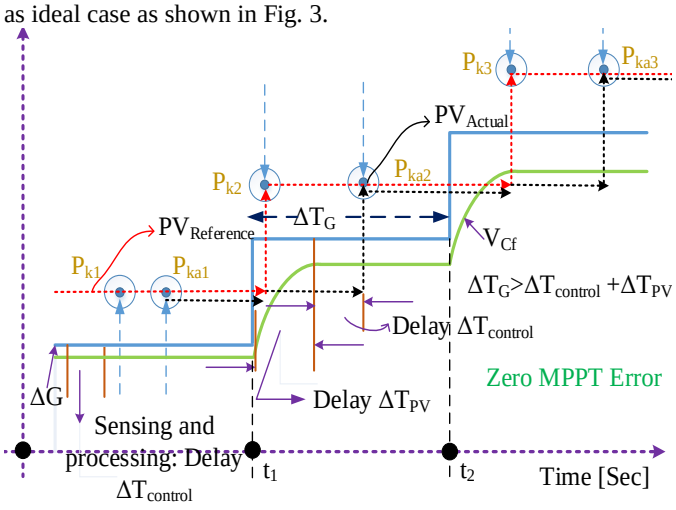

Fig. 3. Ideal MPPT dynamics with zero error under irradiation change, where ΔG is change in irradiation, ΔTpv is time delay due to PV time constant.

A high value of C_f is practically recommended to decoupling the power from the DC side and the AC side and minimize the voltage ripple [10]. However, a large capacitance value increases the source side time constant so that the voltage change is not instantaneous after an irradiation change. Thus, change in control signal (voltage and current) takes time as well as processing the control decision (duty ratio) to track maximum power lags in tracking actual maximum power. This is considered a non-ideal case of tracking maximum power and creates a non-negligible error. From Fig. 4 it is clear that change in irradiation varies reference maximum PV panel power but due to delay in control signal the converter is unable to change duty ratio and hence creates a significant error in tracking maximum power. This problem is more pronounced when irradiation change time is less compared to PV panel time constant with capacitor and MPPT tracking error increases as shown in Fig. 4: The reference power P_{K2} and actual power after MPPT P_{Ka2} are not the same because P_{Ka2} holds the previous power condition as duty ratio does not change. Therefore, the minimum circuit time constant will ensure an accurate MPPT performance. This also eliminates the usage of complex control techniques like adaptive control [15]-[16] etc. for extracting MPP.

A. System dynamics from PV equivalent circuit model

System dynamics under irradiation variation can be derived using an equivalent circuit model of PV. Single diode model [1] of the PV panel

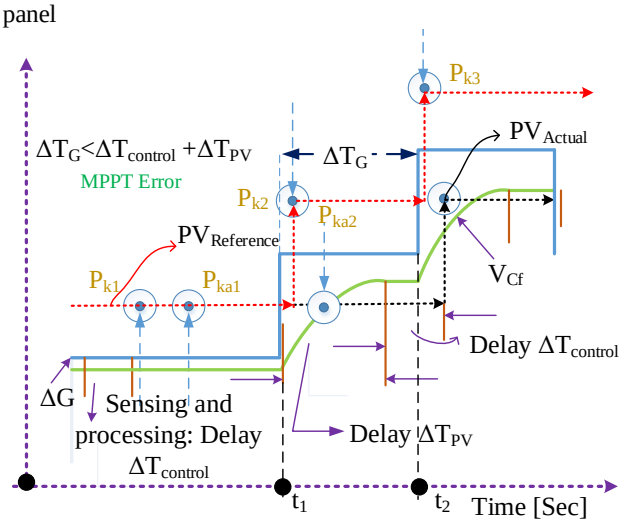

Fig. 4. MPPT dynamics with tracking error under irradiation change, where ΔG is the change in irradiation, ΔTpv is time delay due to PV time constant.

is adopted in this article as shown in Fig. 5. The output current and voltage from one PV cell are $I=I_{ph}-I_d-I_{sh}$ and V respectively.

$$I_d = I_{se}\left[\exp\left(\frac{V+IR_{se}}{nV_t}\right)-1\right],\ I_{sh} = \frac{V+IR_{se}}{R_{sh}}. \quad (1)$$

$$\text{Thus, } I = I_{ph} - I_{se}\left[\exp\left(\frac{V+IR_{se}}{nV_t}\right)-1\right] - \frac{V+IR_{se}}{R_{sh}} \text{ and } V_t = \frac{T_c K}{q} \quad (2)$$

where, q: charge of the electron ($q=1.6\times10^{-19}$C) K: Boltzmann Constant. T: Temperature in K. R_{sh}: Shunt resistance, R_{se}: Series resistance, n: Ideality factor and I_{se}: Reverse bias saturation current.

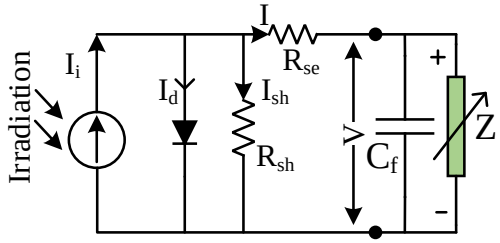

Fig. 5. Single diode model of PV panel.

From the equivalent circuit (Fig. 5) of PV, the voltage and current

This article has been accepted for publication in a future issue of this journal, but has not been fully edited. Content may change prior to final publication. Citation information: DOI 10.1109/JESTPE.2020.2986858, IEEE Journal of Emerging and Selected Topics in Power Electronics

dynamic can be easily derived both in open circuit and loaded condition.

The open circuit PV voltage equation (3) across capacitor (C_f) is

$$v(t)=i_i(t)R_{sh}\left[u(t)-u(t)e^{\frac{-t}{C_f(R_{se}+R_{sh})}}\right] \quad (3)$$

Where, u(t)= Step voltage, v(t)= PV voltage and i_i=PV current source.

The output PV voltage contains steady-state as well as transient information. System dynamics can be expressed by equation (4).

$$v(t)_{transient}=i_i(t)R_{sh}e^{\frac{-t}{C_f(R_{sh}+R_{se})}} \quad (4)$$

Under loading condition, the transient equation (4) can be written as

$$v(t)_{transient}=\frac{i_i(t)}{\left[\frac{1}{R_{sh}}+\frac{1}{Z}\left(1+\frac{R_{se}}{R_{sh}}\right)\right]}e^{\frac{-t(Z+R_{se}+R_{sh})}{C_f Z(R_{sh}+R_{se})}} \quad (5)$$

The transient slope of the PV voltage should be maximum to attain faster transient response under irradiation change and can be derived from equation (4) and (5) which is

$$|M|=\left|\frac{dv_{o\_transient}}{dt}\right|_{t=0}=\frac{i_i(0)R_{sh}}{C_f(R_{sh}+R_{se})}=\frac{I_iR_{sh}}{C_f(R_{sh}+R_{se})} \quad (6)$$

Where $i_i(0)=I_i$.

Short circuit (SC) condition of PV panel provides worst transient performance. However, during MPPT operation of PV converter, the impedance is non-zero. Therefore, designing a maximum M value ensures minimum error in tracking maximum power at rapidly changing environmental conditions. But finding maximum M value requires information about series resistance (R_{se}), shunt resistance (R_{sh}) which are temperature and irradiation dependent.

In this article PV panel parameters are determined through an extraction model originally proposed by J.A.Gow *et.al*. [17], which is accurate for power electronics application. It is described by the following equations.

$$I_i=K_oV(1+K_1T),$$

$$I_d=K_2T^3e^{\left(\frac{K_6}{T}\right)},\ R_{se}=K_3+\frac{K_4}{V}+K_5T,\ R_{sh}=K_8e^{K_9T} \quad (7)$$

Where, K_o=-5.729X10^{-7}, K_1=-0.1098, K_2=44.5355, K_3=1.47, K_4=1.612X10^3, K_5=-4.474X10^{-3}, K_6=-7.31X10^3, K_8=2.303X10^6 and K_9=-2.711X10^{-2}. V= PV Voltage at different temperature (T), irradiation (G), T=Ambient temperature in Kelvin (K).

From equation (6) and (7), the maximum slope (M) of PV panel KC 200GT is calculated which is a function of the irradiation, temperature and different values of C_f. The theoretical results are reported in Fig. 6 where the base value of C_f is taken as 1000μF for calculation.

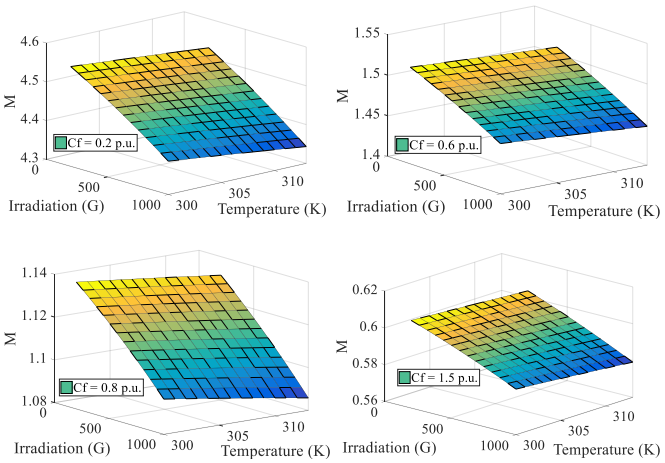

Fig. 6. Change in M with variation in ambient temperature T (K) and solar irradiation G (Watt/m^2) for different capacitor values.

It is evident from Fig. 6 that at C_f=0.2 p.u. the transient delay is least for different temperature (T) and irradiation (G) as the slope (M) is maximum. Similarly, for C_f=1.5 p.u. provides longer transient delay as the slope is very small compared to C_f=0.2 p.u. Thus, theoretically, very low capacitance ensures better MPP tracking performance. However, in practice, the capacitance value should not be too low based on PV panel rating and ripple power effect.

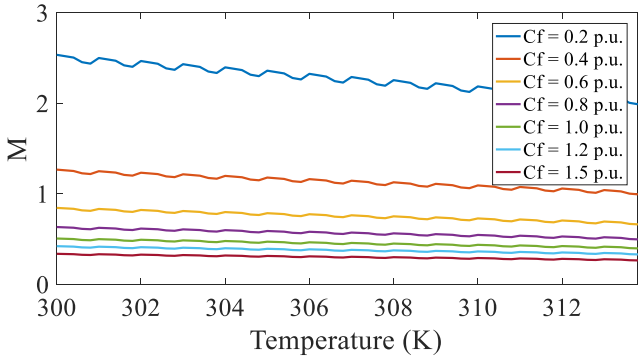

Fig. 7. The value of M at different ambient temperature in Kelvin.

Fig.7 reports the effects of temperature variation on M, considering different p.u. values of C_f. Again, according to Fig.7 low capacitor ensures higher M value for better dynamic response under temperature variation and at constant irradiation. Temperature increment not only degrades PV panel efficiency [1] but also decreases slope (M) which further degrades MPP performance.

B. Ripple power effect on capacitor (C_f) selection:

DC link capacitor (C_o) before H bridge voltage source inverter (VSI) plays an important role in capacitor (C_f) selection as this value can be indirectly determined through comparison of Z_{in} looking from the output terminal of the boost converter. Therefore, the steps are initially to find the optimum value of C_o for minimizing ripple power when VSI is connected to the grid and secondly to find out effective input impedance of boost converter taking the calculated C_o value. Finally comparing (Z_{cdc}) and Z_{in} the accurate capacitor (C_f) value is derived. The system of analysis is shown in Fig. 8 and 10. Line inductance is considered as L_i and S_1-S_4 are MOSFET switches. V_{dc} is the dc-link capacitor voltage.

This article has been accepted for publication in a future issue of this journal, but has not been fully edited. Content may change prior to final publication. Citation information: DOI 10.1109/JESTPE.2020.2986858, IEEE Journal of Emerging and Selected Topics in Power Electronics

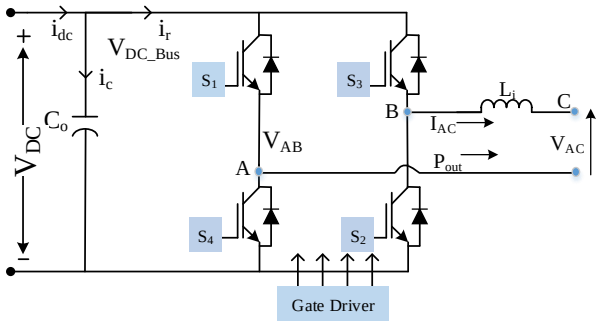

Fig. 8. Single-phase full-bridge inverter.

Let, the low-frequency component output voltage to be sinusoidal and equal to $V_{AB}=V_m \sin \omega t$ and $I_{AC}=I_m \sin(\omega t-\varphi)$ where ω is grid frequency and φ is phase angle difference between V_{AB} and I_{AC}. Thus, the instantaneous power injected to the grid is $P_{out}=V_{AC}I_{AC}$ with $V_{AC}=V_m \sin \omega t-\omega L_i I_m \cos(\omega t-\varphi)$.

The output power can be subdivided into $P_{out}=P_{av}+P_{ripple}$ where if I_{AC} is controlled in phase to V_{ac}

$$P_{av}=\frac{V_m I_m}{2}\cos\varphi \text{ and}$$

$$P_{ripple}=-\frac{V_m I_m}{2}\cos(2\omega t-\varphi)-\frac{\omega L_i I_m^2}{2}\sin(2\omega t-2\varphi) \quad (8)$$

Line inductance is very small and therefore by neglecting it, equation (8) can be rewritten as

$$P_{ripple}=-\frac{V_m I_m}{2}\cos(2\omega t-\varphi)$$
$$=\sqrt{P_{av}^2\left(1-\left(\frac{\sin\varphi}{\cos\varphi}\right)^2\right)}\sin(2\omega t-2\varphi+\psi) \quad (9)$$

Thus $P_{ripple}=B\sin(2\omega t-2\varphi+\psi)$ (10)

Where, $B=\sqrt{P_{av}^2\left(1-\left(\frac{\sin\varphi}{\cos\varphi}\right)^2\right)}$

The voltage ripple of dc-link capacitor is determined from ripple power expression. This voltage ripple contains dominant 2nd order harmonics of line frequency and elimination of this harmonics is essential for successful decoupling between DC to AC side which is still a major problem [18].

Capacitor voltage dynamic equation can be written as,

$$V_{dc}i_{dc}+V_{dc}C_o\frac{dv_{dc}}{dt}=B\sin(2\omega t-2\varphi+\psi)+P_{av} \quad (11)$$

The ripple power creates an extra circulating loss within the boost converter which degrades the life of the PV system. Large capacitors are generally recommended to avoid this effect. The voltage equation across C_o can be obtained by solving,

$$\left.\begin{aligned}P_{cap}=P_r=V_{dc}i_c&=-\frac{V_m I_m}{2}\cos(2\omega t-\varphi)\\ V_{dc}C_o\frac{dv_{dc}}{dt}&=-\frac{V_m I_m}{2}\cos(2\omega t-\varphi)\end{aligned}\right\} \quad (12)$$

The dc-link capacitor voltage as well as the maximum and minimum capacitor voltage result as

$$V_{dc}=\sqrt{\left(N-\frac{V_m I_m}{2C_o\omega}\sin(2\omega t-\varphi)\right)} \quad (13)$$

$$V_{dc\_max}=\sqrt{\left(N+\frac{V_m I_m}{2C_o\omega}\right)} \quad (14)$$

$$V_{dc\_min}=\sqrt{\left(N-\frac{V_m I_m}{2C_o\omega}\right)} \quad (15)$$

Where, $V_{av}=\frac{V_{dc\_max}+V_{dc\_min}}{2}$, $N=V_{av}^2+\left(\frac{V_m I_m}{4V_{av}C_o\omega}\right)^2$

Equations (14) and (15) can be greatly simplified in

$$V_{dc\_max}=V_{av}+\frac{V_m I_m}{4V_{av}C_o\omega} \quad (16)$$

$$V_{dc\_min}=V_{av}-\frac{V_m I_m}{4V_{av}C_o\omega} \quad (17)$$

From equations (16) the range of C_o can be derived

$$C_o\geq\left(\frac{V_m I_m}{4\left(V_{dc\_max}-V_{av}\right)V_{av}\omega}\right) \quad (18)$$

Therefore, the minimum capacitor is

$$C_{o\_min}=\frac{V_m I_m}{\left(V_{dc\_max}^2-V_{dc\_min}^2\right)\omega} \quad (19)$$

Maximum dc-link voltage can be calculated by taking minimum voltage at 1 p.u. for different value of capacitances.

Similarly, from equation (19) the minimum capacitance value is derived which is 0.2724 p.u. for an average voltage of 1.0 p.u. as shown in Fig. 9.

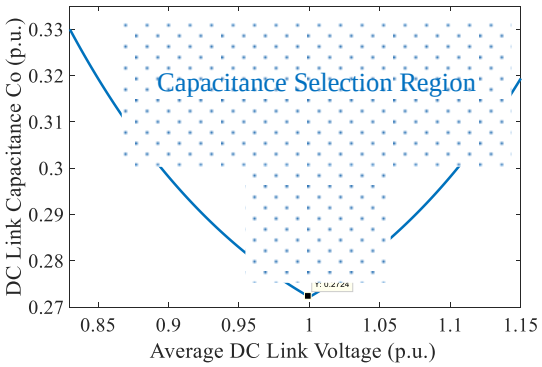

Fig. 9 DC link capacitance (C_o) selection region with minimum capacitance point.

The region above the minimum capacitance point as denoted in the Fig. 9 is capacitor selection region for proper decoupling.

This article has been accepted for publication in a future issue of this journal, but has not been fully edited. Content may change prior to final publication. Citation information: DOI 10.1109/JESTPE.2020.2986858, IEEE Journal of Emerging and Selected Topics in Power Electronics

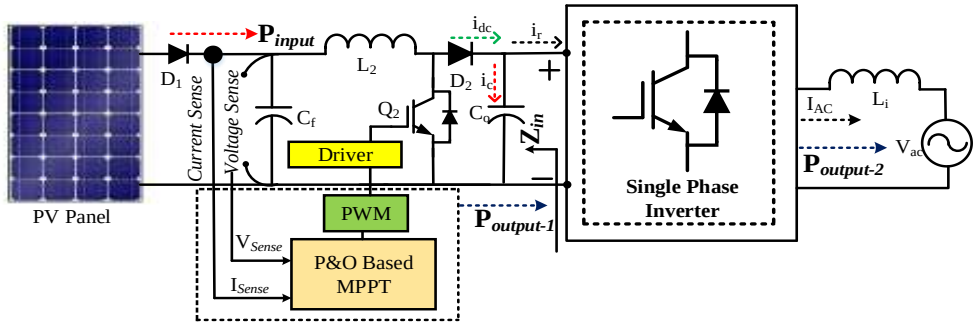

Fig. 10. System arrangement.

Using (12) and (13) the capacitor current (i_c) can be obtained as,

$$i_c = \frac{-\frac{V_m I_m}{2}\cos(2\omega t-\varphi)}{\sqrt{\left[\left(V_{av}+\frac{V_m I_m}{4V_{av}C_o\omega}\right)^2-\frac{V_m I_m}{2C_o\omega}\left(1+\sin(2\omega t-\varphi)\right)\right]}} \quad (20)$$

The dc current (i_{dc}) can be measured by applying KCL at the node of boost converter load which is, $|i_{dc}|=|i_c+i_r|$ as shown in Figs. 8 and 10.

Further, the capacitor current for different capacitor values is determined and plotted as shown in Fig. 11 (a). It is clear from the figure that the capacitor current does not vary much with changing capacitor value at a constant average dc-link voltage. But the capacitor current is prone to change with changes in average dc-link voltage at a constant capacitor value as shown in Fig. 11 (b).

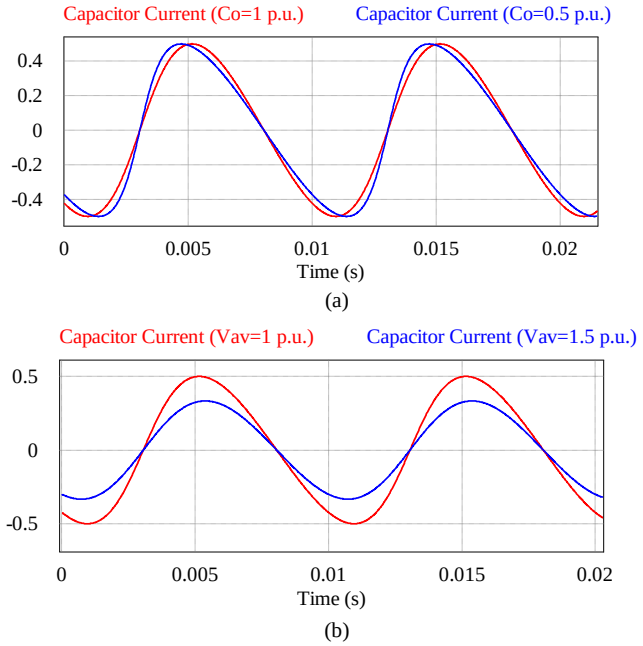

Fig. 11. Capacitor current (in p.u.) variation with (a) capacitance variation with constant dc-link voltage (in p.u.) (b) Variation in average dc link voltage (in p.u.) at constant capacitance.

Again, $I_{AC}=I_m\sin(\omega t-\varphi)$, is only valid if dc link voltage is greater than the maximum value of ac side voltage ($V_{dc}>V_m$). Therefore, 100 Hz ac component ripple can be decoupled with low-value capacitor C_o.

III. Capacitor Selection Method

As per the discussion in PV panel parameter C_f value should be low for accurate MPP extraction under irradiation variation. However, C_o is having a minimum value as given in equation (19) for proper decoupling. Thus, comparing the effective equivalent impedance (Z_{in}) looking from C_o with Z_{Cdc}, the correct C_f value is determined which ensures proper power decoupling and error-free maximum power tracking.

For a boost converter, the input impedance (Z_{in}) depends on the duty ratio (D), C_f and inductor L_2. The R_f value is the combination of R_{se}, R_{sh}, and ESR of inductor L_2.

$$Z_{in}=\frac{1}{D^2}\frac{s^2L_2C_fR_f+sL_2+R_f}{1+sR_fC_f} \quad (21)$$

For large C_f value Z_{in} is dominated by inductor L_2. However, C_f value should not be too high to make error-free power point tracking. Hence input impedance (Z_{in}) is plotted taking C_f=0.2 p.u. and other parameters from TABLE-I with frequency variation greater than 1 kHz. Again, the impedances (Z_{cdc}) of C_{dc} are plotted under different C_{dc} values as per the minimum value requirement as given in equation (19). From Fig. 12, it is clear that the Z_{in} is higher than Z_{cdc} for all frequencies greater than 1 kHz.

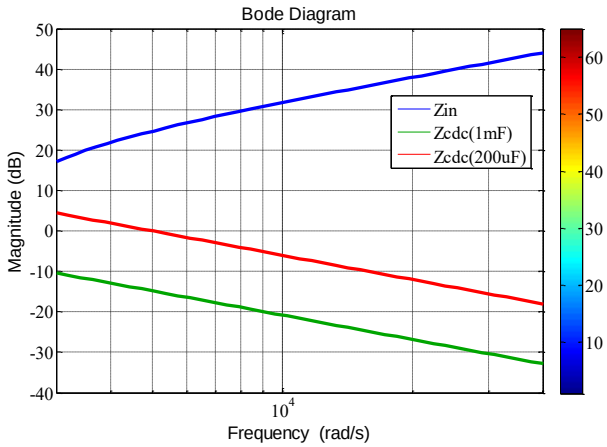

Fig. 12 Input impedance (Z_{in}) of boost converter with impedance (Z_{cdc}) of C_{dc}.

Thus, proper decoupling is achieved from DC to AC side and high-frequency component of the boost converter is bypassed successfully. Therefore, the PV voltage is regulated properly using a DC-DC boost converter with small ripple. This is achieved with full-bridge ac current regulation using small dc-

link capacitor and source-side capacitor value minimization.

The settling time [19] depends on the capacitor value both in MPP region and constant current region (CVR) which are respectively,

$$T_{\Delta} = -\frac{1}{\xi_{PV}\omega_n}\ln\left(\Delta\sqrt{1-\xi_{PV}^2}\right) \quad (22)$$

$$\text{And } T_{\Delta} = -\frac{1}{\xi_{PV}\omega_n}\ln\left(\frac{\Delta}{2}\sqrt{1-\xi_{PV}^2}\right) \quad (23)$$

$$\text{Where } \xi_{PV} \approx \frac{1}{2}\left(\frac{1}{r_{pv}}\sqrt{\frac{L_2}{C_f}} + R_f\sqrt{\frac{C_f}{L_2}}\right) \text{ and } \omega_n \approx \frac{1}{\sqrt{L_2 C_f}}$$

The worst dynamic performance of PV is at short circuit condition, therefore ζ_{PV} at short circuit (SC) condition is the guiding parameter of selecting perturbation frequency.

$$\xi_{PV\_SC} \approx \frac{R_f}{2}\sqrt{\frac{C_f}{L_2}} \quad (24)$$

Therefore, the perturbation time interval (ΔT) should be greater than TΔ in short circuit (SC).

$$|\Delta T\rangle |T_{\Delta}| = \frac{1}{\xi_{PV\_SC}\omega_n}\ln\left(\Delta\sqrt{1-\xi_{PV\_SC}^2}\right) \quad (25)$$

Thus, for low capacitor value, the settling time becomes lower and low perturbation frequency can effectively track the MPP under steady and dynamic condition.

Finally, the low capacitance at source side (C_f) and dc-link capacitance (C_o) ensures correct MPP tracking of PV and successful decoupling of DC to AC side. The system configuration to validate the theoretical finding is mentioned in TABLE-I.

TABLE-I
SYSTEM CONFIGURATION

Components	Parameters	Part Number
PV Panel (One Unit)	V_{oc}=32.9 V, I_{sc}=7.61 A P_{max}=200 W	KC 200GT
Boost Converter	V_{in}=20 to 40 V V_o=80 V , L_2= 1mH C_o =400uF , C_f=200uF f_{sw}=10kHz	**MOSFET**: IRF640 **Ferrite Cor**e: PQ **Optocoupler** (6N137) **based Gate Driver**: IR2110
H bridge Inverter	PWM method= Sin-triangle PWM Carrier Frequency (f_c)=5 kHz 1kVA	MOSFET: IRF 640 Gate driver: IR2110
Central Controller for boost converter and H bridge Inverter	Programming in Lab-View Scan Interface.	NI cRIO 9082 Module: NI 9401, NI 9227 (current sensor) NI9225 (Voltage Sen sor)
PV interfaced capacitor (C_f)	C_f=200 uF@ 350V, 1000uF@450V (Electrolytic)	ST1047, H045
Transformer	Step-Up type, 1kVA	Turns Ratio (1:5)

The performance of proposed error-free maximum PV power extraction system with correct capacitance value is compared with existing techniques like adaptive control, flexible multi-MPPT control, though all the existing methods are based on control techniques.

TABLE-II
PERFORMANCE COMPARISON

Methods	Processing Delay & Hardware Complexity	Settling Time (Sec)	Tracking Error*
PV Micro inverter with P& O algorithm [3]	High Low ADC requirement (Approx 10kspa) **Computational Barden**: Low	Min-6.5	≈16-17%
PV Microinverter with adaptive P&O control [10]	Medium Fast ADC Rrquirement. (Approx.30ksps) **Computational Barden**: Medium	Min-0.034 Max-5.1	1-2%
Flexible Multi-MPPT Control. [20]	Medium Fast ADC Rrquirement. (Approx.30ksps) **Computational Barden**: High	Min-3.0	Medium
Adaptive FPPT Control [7]	Medium Fast ADC Rrquirement. (Approx.30ksps) **Computational Barden**: High	Min-1.2 Max-10.5	Min-3.3% Max-14.4%
Proposed capacitor selection-based P&O MPPT.	Low Low ADC requirement (Approx 10kspa) **Computational Barden**: Low	Min-2.4	Min-2.9%

$$\text{* Tracking Error} = \frac{\int |P_{PV} - P_{MPP}|}{\int |P_{PV}|} \times 100\ \%$$

From TABLE-II, it is clear that all the existing methods for tracking error-free maximum power are based on advanced control techniques. These control techniques increase computation burden and do not guarantee a zero error maximum power extraction under the changing environment as they are based on same voltage and current dynamics. The proposed technique guarantees true error-free power extraction as voltage and current dynamic changes quickly as per change in irradiation and temperature.

IV. Results and Discussion

From the previous discussion, it is clear that for low capacitance value ensures better performance of MPP tracking from PV under varying environmental conditions. It also confirms better performance at low perturbation frequency when a perturbation-based technique is used for extracting maximum power. PSIM 9.1.1 software platform is used for simulating of the proposed system and 500W practical PV laboratory prototype system is used for validating the proposal. From Figs. 13 (a) and (b) it is evident that MPP performance is better at C_f=0.2 p.u. than C_f=1.0 p.u. case.

This article has been accepted for publication in a future issue of this journal, but has not been fully edited. Content may change prior to final publication. Citation information: DOI 10.1109/JESTPE.2020.2986858, IEEE Journal of Emerging and Selected Topics in Power Electronics

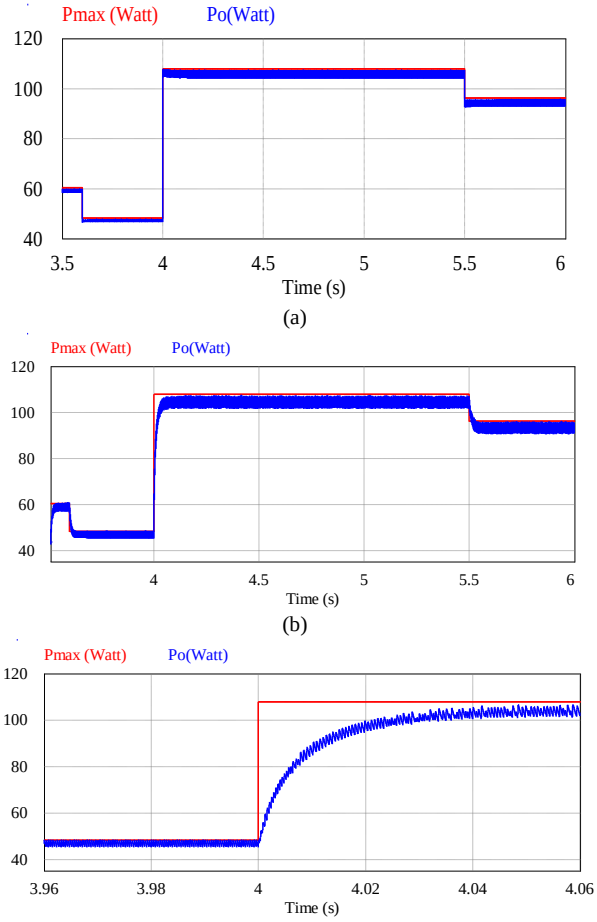

Fig. 13 (a) Power point tracking with C_f=0.2 p.u. (b) Power point tracking with C_f=1 p.u. (c) Zoomed view at t=4sec in power point tracking with C_f =1.0 p.u.

Delay is higher with high C_f in MPP tracking. The high capacitor takes a larger time to settle the new voltage value as shown in Fig. 14 (a) during irradiation change at 4 sec whereas the voltage change is almost immediate at low C_f. Therefore, the MPP error is greater with a large value of capacitor (C_f).

The proposed concept is applied in 500W prototype PV panel system as shown in Fig. 15. The control environmental condition is designed using NI-cRIO 9082.

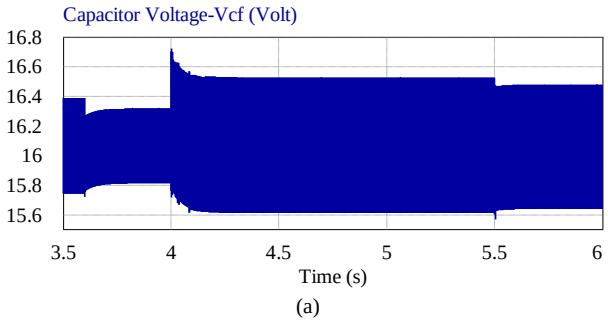

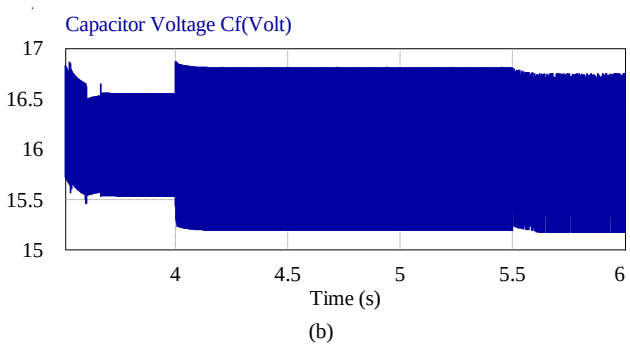

Fig. 14 (a) Capacitor voltage for C_f=1.0 p.u. (b) Capacitor Voltage for C_f= 0.2 p.u.

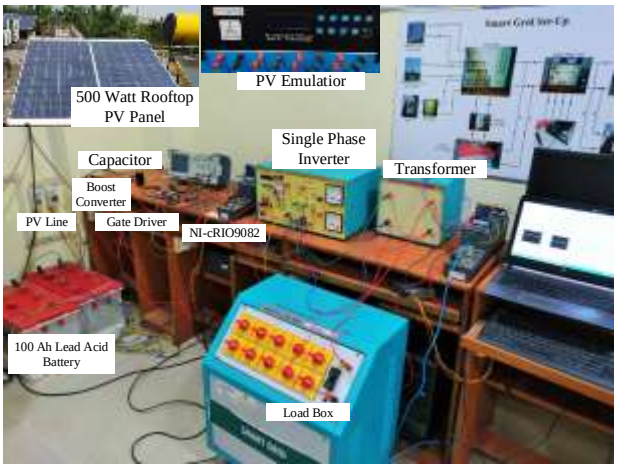

Fig.15 Hardware set up.

The MPP power is calculated by measuring PV voltage (V_{cf}) and current. Temperature effect is ignored as temperature is almost constant during measurement. MPP tracking performance is tested for different irradiation variations (600W/m^2-500W/m^2-400W/m^2-800W/m^2-600W/m^2) with low capacitance (C_f=0.2 p.u.) as shown in Fig. 16 (b). Under the same conditions, the tracking performance degrades with higher capacitance (C_f=1.0 p.u.) as shown in Fig. 16 (a).

The practical results as shown in Figs. 16 (a) and (b) confirms that MPP error is less with low capacitance i.e. at C_f =0.2 p.u compared to C_f=1.0 p.u. The hardware result matches with the simulated results.

Perturb and observe (P and O) MPPT method is tested at a step irradiation changes from 300 W/m^2 to 1000 W/m^2 with higher capacitance and lower capacitance. It is found that the same P and O MPPT algorithm performs better as settling time is less (2.4 sec) with lower capacitance (C_f=0.2p.u.) compared to higher capacitance (C_f=1p.u.) as shown in Figs. 17 (a) and (b). Fig. 17 (c) shows a better tracking performance under a pulse irradiation variation.

This article has been accepted for publication in a future issue of this journal, but has not been fully edited. Content may change prior to final publication. Citation information: DOI 10.1109/JESTPE.2020.2986858, IEEE Journal of Emerging and Selected Topics in Power Electronics

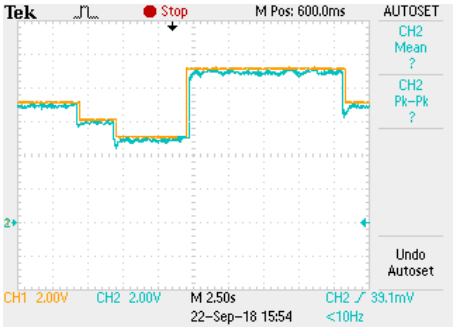

(a)

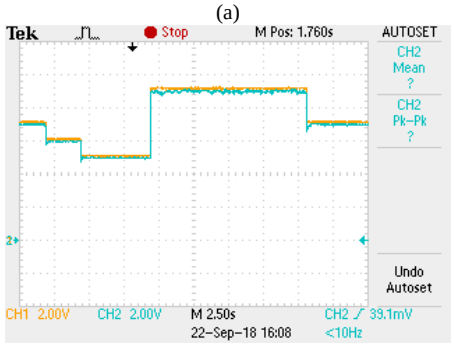

(b)

Fig. 16 Maximum power point (MPP) tracking performance (a) with C_f=1.0 p.u. (b) with C_f=0.2 p.u. **Y Axis**: [**Yellow-P_{MPP}** Maximum power point, **Blue-PV available power**] (**20 Watt/div**), **X Axis**: Time (**2.5s/div**)

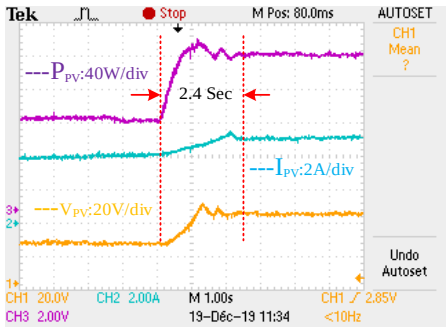

(a)

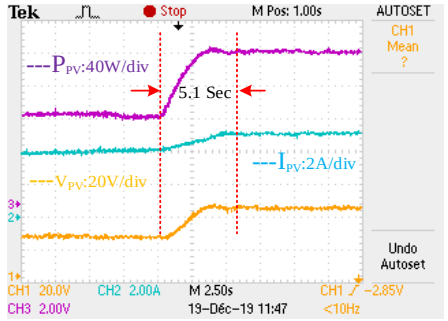

(b)

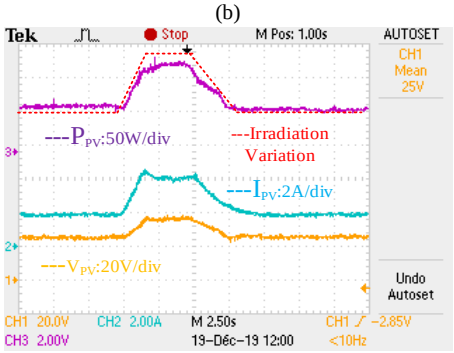

(c)

Fig. 17 P&O Performance at step irradiation change (300 W/m2-1000W/m^2) with different capacitance (a) C_f=0.2p.u. (b) C_f=1.0p.u. (c) Better tracking performance with Cf=0.2 p.u. (300 W/m^2-700 W/m2-300 W/m^2).

Another testing (step change of irradiation from 300 W/m^2-1000W/m^2) is performed implementing incremental conduction (IC) method of MPPT for performance verification with lower value of capacitance. The settling time is less i.e. 2.1 sec for lower capacitance (C_f=0.2p.u.) whereas it is higher i.e. 4.9 sec for higher capacitance (C_f=0.2p.u) in IC method of MPPT.

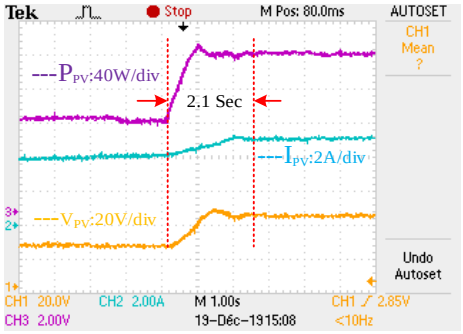

(a)

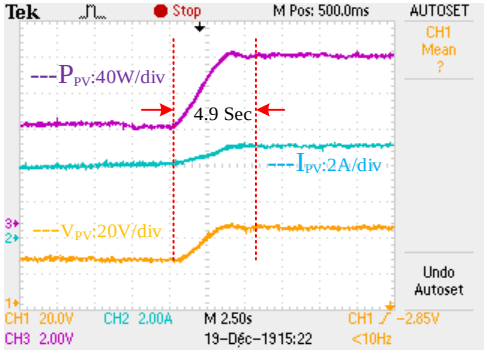

(b)

Fig. 18 IC Performance at step irradiation change (300 W/m^2-1000W/m^2) with different capacitance (a) C_f=0.2p.u. (b) C_f=1.0 p.u.

A comparison is performed with P & O and IC method as mentioned in TABLE-III, which confirms betterment in settling time and error tracking performance with using low capacitance value.

TABLE-III
PERFORMANCE COMPARISON

Methods	Settling Time (Sec)	Tracking Error*
P & O Method with C_F=0.2 p.u.	≈2.4	2.9%
P & O Method with C_F=1.0 p.u.	≈5.1	6.8%
IC Method with C_F=0.2 p.u.	≈2.1	2.74%
IC Method with C_F=1.0 p.u.	≈4.9	6.47%

The error in tracking MPP increases with a higher capacitance value as shown in Fig. 19.

This article has been accepted for publication in a future issue of this journal, but has not been fully edited. Content may change prior to final publication. Citation information: DOI 10.1109/JESTPE.2020.2986858, IEEE Journal of Emerging and Selected Topics in Power Electronics

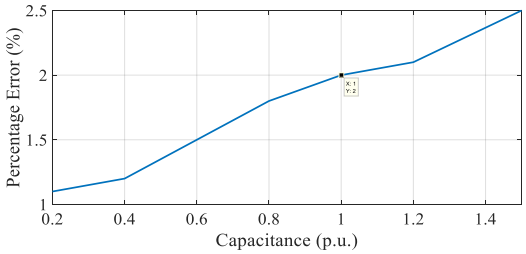

Fig. 19 MPP Error for different (C_f) in p.u. @ 500W PV Panel.

However, low capacitance value has a restriction in practical application based on the power of PV system. For a small power PV system, a low capacitance value is suitable. As shown in TABLE-IV the preferable design of PV based power extraction system is simulated and tested.

TABLE -IV
CAPACITOR SELECTION VALUE WITH WATTAGE AND ERROR

Capacitor Selection value (Electrolytic)	Power of the System	Irradiation Variation	Error
1000uF (Simulated)	4000W	800-1000 watt/m^2	72W
1000uF (Simulated)	2000W	800-1000 watt/m^2	42W
800uF (Simulated)	1200W	800-1000 watt/m^2	30.5 W
800uF (Simulated)	1000W	800-1000 watt/m^2	24W
200uF @ 350Volt (Simulated and Tested)	500W	800-1000 watt/m^2	6W

The MPPT performance at partial shading condition is tested with C_f=200µF. Two 250 Watt PV panels are connected in series with uniform irradiation at 800 W/m^2. Irradiation is changed to 200 W/m^2 in one panel during operation to achieve partial shading effect. The power extraction performance at shaded condition with C_f=0.2 p.u is better compared to high C_f=1.0 p.u. as shown in Figs. 20 (a) and (b).

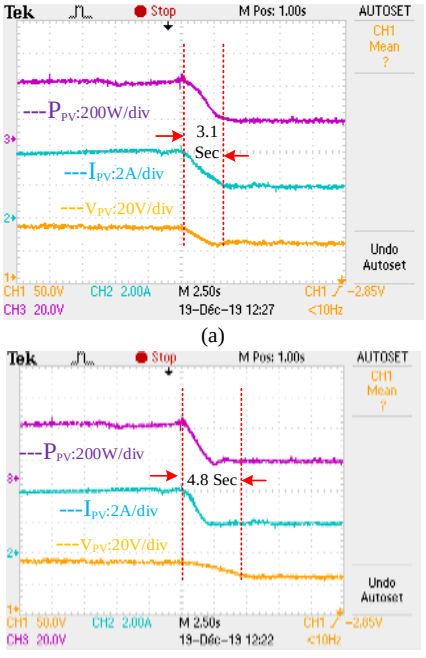

Fig. 20 PV output at partial shading (a) with C_f= 0.2 p.u. (b) with C_f=1.0 p.u

As P & O algorithm fails to track the global maximum point (GMP) under partial shading therefore better algorithm with low capacitance (C_f) value performs better in terms of tracking GMMP.

V. Conclusion

This work analyses the impact of capacitor (C_f) on MPPT performance of PV panel using fixed perturbation frequency under irradiation and temperature variation. The capacitor (Cf) value is selected based on parameters like maximizing M, settling time and ripple power. This selection further confirms the perturbation frequency which guarantees accurate MPP tracking under varying environmental conditions. Based on 500W prototype study, it is found that in an average extra 4.5W power is lost if C_f value is selected as 1000µF instead of 200µF. Again, with low capacitance (C_f) value reduces the settling time in each perturbation. Therefore, perturbation frequency can be limited to extract correct MPP for different environmental conditions.

References

[1] Yongheng Yang, Katherine A. Kim, Frede Blaabjerg, and Ariya Sangwongwanich "*Advances in Grid-Connected Photovoltaic Power Conversion Systems*", 1st edition, Woodhead Publishing, Aug. 2018.

[2] C.S. Solanki, "*Solar Photovoltaics Fundamentals, Technologies and Applications*", 2nd edition, New Delhi, India: PHI Learning Private Limited, 2011.

[3] D. Sera, T. Kerekes, R. Teodorescu, and F. Blaabjerg, "Improved MPPT method for rapidly changing environmental conditions," *IEEE International Symposium on Industrial Electronics*, Montreal, Que., 2006, pp. 1420-1425.

[4] D. Sera, R. Teodorescu, J. Hantschel, and M. Knoll, "Optimized Maximum Power Point Tracker for Fast-Changing Environmental Conditions," in *IEEE Transactions on Industrial Electronics*, vol. 55, no. 7, pp. 2629-2637, July 2008.

[5] G. Escobar, S. Pettersson, C. N. M. Ho, and R. Rico-Camacho, "Multisampling Maximum Power Point Tracker (MS-MPPT) to Compensate Irradiance and Temperature Changes," in *IEEE Transactions on Sustainable Energy*, vol. 8, no. 3, pp. 1096-1105, July 2017.

[6] S.B.Santra, D.Chatterjee, S.Banerjee, K.Kumar, and M. Bertoluzzo, "Selection of Capacitor in PV System for Maximum Power Point Tracking", in *Proceedings of IEEE International Conference on Power Electronics, drives and energy systems* (PEDES-2018), IIT Madras, India, Dec-2018. ISBN: 978-1-5386-9316-2/18/$31.00 ©2018 IEEE.

[7] H. Dehghani Tafti, A. Sangwongwanich, Y. Yang, J. Pou, G. Konstantinou, and F. Blaabjerg, "An Adaptive Control Scheme for Flexible Power Point Tracking in Photovoltaic Systems," in *IEEE Transactions on Power Electronics*. 34, no. 6, pp. 5451-5463, June 2019.

[8] Tafti, Hossein Dehghani, et al. "A Multi-Mode Flexible Power Point Tracking Algorithm for Photovoltaic Power Plants." *IEEE Transactions on Power Electronics*, Vol. 34, no.6, pp. 5038-5042, June 2019.

[9] W. Feng, et al. "An Improved Submodule Differential Power Processing-Based PV System with Flexible Multi-MPPT Control." *IEEE Journal of Emerging and Selected Topics in Power Electronics*, vol.6, no.1, pp. 94-102, March 2018.

[10] S. Sankar, et al. "High-Speed Maximum Power Point Tracking Module for PV Systems." *IEEE Transactions on Industrial Electronics*, vol. 66, no.2, pp. 1119-1129, Feb 2019.

[11] H. Hu, S. Harb, N. Kutkut, I. Batarseh, and Z. J. Shen, "A Review of Power Decoupling Techniques for Microinverters With Three Different Decoupling Capacitor Locations in PV Systems," *IEEE Transactions on Power Electronics*, vol. 28, no. 6, pp. 2711-2726, June 2013.

[12] R. W. Erickson and A. P. Rogers, "A Microinverter for Building-Integrated Photovoltaics," 24th Annual IEEE *Applied Power Electronics*

Conference and Exposition, Washington, DC, 2009, pp. 911-917. doi: 10.1109/APEC.2009.4802771.

[13] S. Jiang, D. Cao, Y. Li, and F. Z. Peng, "Grid-Connected Boost-Half-Bridge Photovoltaic Microinverter System Using Repetitive Current Control and Maximum Power Point Tracking," in *IEEE Transactions on Power Electronics*, vol. 27, no. 11, pp. 4711-4722, Nov. 2012.

[14] N. Femia, G. Petrone, G. Spagnuolo, and M. Vitelli, "*Power Electronics and Control Techniques for Maximum power harvesting in Photovoltaic System*" Boca Raton, FL, USA: CRC Press, 2013.

[15] Yang, Y, Wen, H., "Adaptive perturb and observe maximum power point tracking with current predictive and decoupled power control for grid-connected photovoltaic inverters", *Journal of Modern Power System And. Clean Energy*, vol. 7, no.2, pp.422-432, March 2019.

[16] L. Piegari, R Rizzo; I. Spina; and P. Tricoli, "Optimized Adaptive Perturb and Observe Maximum Power Point Tracking Control for Photovoltaic Generation." *Energies*, vol.8, no.5, pp. 3418-3436, April 2015.

[17] J. A. Gow and C. D. Manning, "Development of a photovoltaic array model for use in power-electronics simulation studies," in *IEE Proceedings - Electric Power Applications*, vol. 146, no. 2, pp. 193-200, Mar 1999.

[18] T. Shimizu, Y. Jin, and G. Kimura, "DC ripple current reduction on a single-phase PWM voltage-source rectifier," in *IEEE Transactions on Industry Applications*, vol. 36, no. 5, pp. 1419-1429, Sept.-Oct. 2000.

[19] J. Kivimäki, S. Kolesnik, M. Sitbon, T. Suntio, and A. Kuperman, "Revisited Perturbation Frequency Design Guideline for Direct Fixed-Step Maximum Power Point Tracking Algorithms," in *IEEE Transactions on Industrial Electronics*, vol. 64, no. 6, pp. 4601-4609, June 2017.

[20] Hu, Jiefeng, et al. "A model predictive control strategy of PV-Battery microgrid under variable power generations and load conditions." *Applied Energy*, vol. 221, pp. 195-203, July 2018.

Subhendu Bikash Santra (M-15): Subhendu Bikash Santra was born in West Midnapur, West Bengal, India in 1989. He received M.E degree from Jadavpur University, Kolkata, India in 2012 where he is currently working toward the Ph.D. degree, all in electrical engineering. He was a Institute Research Scholar in Power Electronics in IIT-Kharagpur in Electrical Engineering dept. during 2013-2014.From, 2014-2015 he was working as an Electrical Engineer (E&M) in Rail Vikas Nigam Limited (*Schedule A PSU under Ministry of Railways, Govt. Of India*) where he designed Earth Mat for Elevated Metro Station and Lightning Protection for Station building.

Presently, Mr. Santra is working as an Assistant Professor in the School of Electrical Engineering in KIIT Deemed to be University, Bhubaneswar, India. He is a Member of IEEE, Institution of Engineers [India] and reviewer of IEEE Transaction on Industrial Electronics, Power Electronics, Vehicular Tech., IET Power Electronics, and IEEE ACCESS Journals. He received "Young Researcher Award" in Electrical Engineering in 2018. His main research interest include Topologies of DC to DC converter in Renewable Energy Application, High Power Density Converter, Control of Power Converters and PMSM/BLDC Motor Drive.

Debashis Chatterjee: was born in Kolkata, India in 1969. He received the Bachelor degree from Jadavpur University, Kolkata, India in 1990, M.Tech. degree from IIT, Kharagpur, India in 1992 and Ph.D degree from Jadavpur University, Kolkata, India in 2005, all in Electrical Engineering. From 1992-2002 he worked as a Sr. Design Engineer in NELCO and Cropmton Greaves Ltd. in industrial drives and automation division and then in Philips India Ltd. as Asst. Manager Lighting Electronics Design.

He is currently a Professor in the Department of Electrical Engineering, Jadavpur University, Kolkata, India. His research interests include electrical machines, variable-speed drives, electric vehicles, renewable-energy generation, and power quality study.

Kundan Kumar was born in Godda, India, in 1984. He received the M. Tech. degree from National Institute of Technology Jamshedpur, Jamshedpur, India, and the Ph.D. degree from the University of Padova, Padova, Italy, both in Electrical Engineering, in 2010 and 2016, respectively. He is currently working as an Assistant Professor with the School of Electrical Engineering, Kalinga Institute of Industrial Technology, deemed to be university, Bhubaneswar, India. His research interests include Electric Vehicles and its charging infrastructures, application of wide bandgap semiconductor devices, Isolated DC–DC Converters.

Dr. Kumar was the recipient of Silver Medal for securing first position during his M. Tech. course and Best Presentation Recognition award at IECON, Japan in 2015. He is a member of IEEE and the Institution of Engineers, India and the Reviewer of IEEE Trans. on Industrial Electronics, Power Electronics, Transportation and Electrification, and Journal of Emerging and Selected Topics in Power Electronics.

Manuele Bertoluzzo received the M.S. degree in electronic engineering and Ph.D. degree in industrial electronics and computer science from the University of Padova, Padova, Italy, in 1993 and 1997, respectively. From 1998 to 2000, he was a member of the Research and Development Division of an electric drive factory. In 2000, he joined the Department of Electrical Engineering, University of Padova, as a Researcher in the Scientific Disciplines' Group "electric converters, machines, and drives." Since 2015, he has been an Associate Professor of systems for automation and of electric road vehicle for graduate students. He is currently involved in the analysis and design of power electronics and control systems for wireless power transfer systems. Dr. Bertoluzzo was the recipient of the 2016 Best Paper Award from the IEEE TRANSACTIONS ON INDUSTRIAL ELECTRONICS.

Ariya Sangwongwanich (S'15-M'19) received the M.Sc. and Ph.D. degree in energy engineering from Aalborg University, Denmark, in 2015 and 2018, respectively. Currently, he is working as a Postdoc Fellow at the Department of Energy Technology, Aalborg University. He was a Visiting Researcher with RWTH Aachen, Aachen, Germany from September to December 2017. His research interests include control of grid-connected converter, photovoltaic systems, reliability in power electronics and multilevel converters. In 2019, he received the Danish Academy of Natural Sciences' Ph.D. prize and the Spar Nord Foundation Research Award for his Ph.D. thesis.

Frede Blaabjerg (S'86–M'88–SM'97–F'03) was with ABB-Scandia, Randers, Denmark, from 1987 to 1988. From 1988 to 1992, he got the PhD degree in Electrical Engineering at Aalborg University in 1995. He became an Assistant Professor in 1992, an Associate Professor in 1996, and a Full Professor of power electronics and drives in 1998. From 2017 he became a Villum Investigator. He is honoris causa at University Politehnica Timisoara (UPT), Romania and Tallinn Technical University (TTU) in Estonia.

His current research interests include power electronics and its applications such as in wind turbines, PV systems, reliability, harmonics and adjustable speed drives. He has published more than 600 journal papers in the fields of power electronics and its applications. He is the co-author of four monographs and editor of ten books in power electronics and its applications.

He has received 32 IEEE Prize Paper Awards, the IEEE PELS Distinguished Service Award in 2009, the EPE-PEMC Council Award in 2010, the IEEE William E. Newell Power Electronics Award 2014, the Villum Kann Rasmussen Research Award 2014, the Global Energy Prize in 2019 and the 2020 IEEE Edison Medal. He was the Editor-in-Chief of the IEEE TRANSACTIONS ON POWER ELECTRONICS from 2006 to 2012. He has been Distinguished Lecturer for the IEEE Power Electronics Society from 2005 to 2007 and for the IEEE Industry Applications Society from 2010 to 2011 as well as 2017 to 2018. In 2019-2020 he serves a President of IEEE Power Electronics Society. He is Vice-President of the Danish Academy of Technical Sciences too. He is nominated in 2014-2019 by Thomson Reuters to be between the most 250 cited researchers in Engineering in the world.